WARSAW UNIVERSITY OF TECHNOLOGY Index 351733
FACULTY OF CIVIL ENGINEERING
COMMITTEE FOR CIVIL AND WATER ENGINEERING
POLISH ACADEMY OF SCIENCES ISSN 1230-2945

DOI: 10.24425/ace.2025.154132
ARCHIVES OF CIVIL ENGINEERING
Vol. LXXI ISSUE 2 2025
pp. 473–489

© 2025. Sławomir Onopiuk, Adam Stolarski, Ryszard Rekucki.

This is an open-access article distributed under the terms of the Creative Commons Attribution-NonCommercial-NoDerivatives License (CC BY-NC-ND 4.0, https://creativecommons.org/licenses/by-nc-nd/4.0/), which permits use, distribution, and reproduction in any medium, provided that the Article is properly cited, the use is non-commercial, and no modifications or adaptations are made.

Research paper

Numerical prognosis of the dynamic response of the steel rectangular slab under the explosive load

Sławomir Onopiuk[1], Adam Stolarski[2], Ryszard Rekucki[3]

Abstract: The paper presents the methodology for determination the numerical prognosis of the dynamic response of the rectangular steel slab subjected to an explosive load, aimed at thorough preparation of experimental tests. In the presented work, in order to fully describe the parameters of the shock wave impact on the steel slab, an appropriate combination of formulas known in the literature was used. In order to describe the dynamic behavior of the rectangular steel slab, the resources of the ABAQUS computing software were used. The Johnson–Cook constitutive model was used to describe the dynamic behavior of the structural material. An explicit procedure has been used to solve the equations of motion for the slab. The parameters of the shock wave from the explosion of the TNT charge with the assumed mass and the distance of its location from the slab were determined. As a result of the numerical analysis, the results of changes in displacement and acceleration in time were presented, indicating the nature of the very intense and fast-varying dynamic behavior of the slab. Conclusions were also formulated regarding the requirements for the selection of parameters of the sensors recording both the function of real explosion pressure in time and the function of acceleration in time of the slab model during experimental tests.

Keywords: damping, dynamic deformation process, explosive load, numerical analysis, steel slab

[1]PhD., Eng., Military University of Technology, Faculty of Civil Engineering and Geodesy, 2 gen. Sylwestra Kaliskiego Street, 00-908 Warsaw 46, Poland, e-mail: slawomir.onopiuk@wat.edu.pl, ORCID: 0000-0002-4533-1271
[2]Prof., DSc., PhD., Eng., Military University of Technology, Faculty of Civil Engineering and Geodesy, 2 gen. Sylwestra Kaliskiego Street, 00-908 Warsaw 46, Poland, e-mail: adam.stolarski@wat.edu.pl, ORCID: 0000-0002-4754-3067
[3]MSc, Eng., Military University of Technology, Faculty of Civil Engineering and Geodesy, 2 gen. Sylwestra Kaliskiego Street, 00-908 Warsaw 46, Poland, e-mail: ryszard.rekucki@wat.edu.pl, ORCID: 0000-0002-2040-7073

www.czasopisma.pan.pl PAN POLSKA AKADEMIA NAUK www.journals.pan.pl

1. Introduction

The scope of the work applies to the numerical prognosis of the dynamic response of the steel rectangular slab under the explosive load, aimed at thorough preparation of experimental tests. The basis for the motivation to take up the topic was the authors' belief that conducting extremely expensive experiments in the field of testing the dynamic reaction of steel slabs subjected to an explosive load in free air cannot be effectively carried out without an appropriate numerical prognosis.

Effective development of such a prediction requires the following components of the solution to be considered:

- Modeling of the explosive load on the basis of experimentally verified procedures.
- Modeling the behavior of the structural element, rectangular steel slab enabling the analysis of fast-changing and short duration dynamic processes.
- Constitutive modeling of the construction material dynamic behavior, taking into account the strengthening of dynamic strength.

The area of knowledge in the field of explosive load modeling is developed in the close circle of researchers and specialists.

The work of Karlos and Solomos [1] presents an overview of the procedures for determining the explosion load on structures in the form of a technical guide. Practical methods of estimating the blast loading on structures are given. Examples of structures subjected to explosive loads were also analyzed.

In the work of Trzciński [2], the comparative analysis of the basic parameters of blast waves, amplitude and specific impulse, obtained with the use of various empirical formulas, was carried out.

In the work of Sochet et al. [3] presents the formulas defining the characteristic parameters of the incident shock wave: the overpressure value, the duration and the overpressure impulse. The researches were carried out for three different explosives: TriNitroToluene (TNT), PEntaerythritol TetraNitrate (PETN) and Ammonium Nitrate / Fuel Oil (ANFO), for which appropriate energy equivalents were determined.

In the work of Siwiński and Stolarski [4], the method of determining the action of an external explosion on building barriers on the basis of the analysis of selected procedures known from the literature, was presented. The algorithm for determining the initial pressure of the incident and reflected wave, the duration of the overpressure and the negative pressure phases as well as the course of pressure load variability over time was developed.

In the field of modeling the behavior of explosively loaded structural elements, computational methods based on system software are used.

For example, in the work by Niezgoda et al. [5], the LS-DYNA computing system was used for the dynamic analysis of a multi-layer energy-absorbing panel with a protective aluminum plate and a supporting steel plate, with dimensions $550 \times 550 \times 2$ mm, loaded with a shock wave from the explosion of a 0.5 kg mass TNT charge, placed centrally over the plate at a distance of 430 mm. As a result of the numerical analysis, the authors found a very good agreement with the obtained results of experimental studies.

In the paper by Trajkovski et al. [6], the LS-DYNA system was also used for a comparative analysis of the load capacity of floors in light armored vehicles (LAVs) subjected to the impact of blast waves from the explosion. The authors showed that a V-shaped hull floor provided a much better vehicle response to explosives than a flat floor.

In the paper by Park and Cho [7], the MSC/DYTRAN computing system was used for numerical validation of the computational method of rectangular unstiffened and stiffened plates under explosive load on the basis of experimental data. Parametric tests for various plate models made it possible to derive design relationships between permanent damage to the plates and the explosive impact parameter. The comparative analysis confirmed the high agreement of the approximation of the experimental results based on the proposed design relationships in comparison to the results obtained for other design formulas known from the literature.

In the work of Zheng et al. [8], the results of experimental tests of square, fully clamped ribbed plates as outer walls of a cuboidal chamber subjected to an internal explosive load, are presented. Based on experimental observations of plate behavior mechanisms, analytical rigid-plastic and elastic-plastic models were presented to calculate the dynamic response and permanent displacements of the plates. Numerical simulations were also carried out using the ANSYS AUTODYN computational software to study the influence of the material strain rate and boundary conditions on the dynamic response of the ribbed plates.

In the presented work, in order to fully describe the parameters of the shock wave impact on the steel slab, an appropriate combination of formulas known in the literature was used. To determine the incident overpressure wave and the duration of the overpressure phase, the formulas according to [3] were used, in which both the overpressure amplitude and the very short duration of the overpressure phase were relatively accurately described. In turn, the incident wave front speed was determined according to the work of Krzewiński [9]. Then, commonly known formulas according to [1, 4] were used to determine the overpressure on the front of the wave reflected from the slab. Finally, the remaining parameters of the blast wave, i.e. the minimum negative pressure below atmospheric pressure, the duration of the negative pressure phase to reach the minimum negative pressure and the duration of the entire negative pressure phase, were determined as a function of the pressure wave variation over time using the expression proposed by Lee and Chiu [10]. Detailed values of the explosion parameters of various explosives are included in the monograph by Cudziło et al. [11].

In order to describe the dynamic behavior of the rectangular steel slab, the resources of the ABAQUS computing software were used [12]. Namely, a computational model of the slab was developed using shell finite elements. The Johnson–Cook constitutive model [13, 14], was used to describe the dynamic behavior of the structural material. An explicit procedure has been used to solve the equations of motion for the slab, see Wriggers' monograph [15], which also contains detailed information on the methods used in nonlinear finite element analysis.

The parameters of the shock wave from the explosion of the TNT charge with the assumed mass and the distance of its location from the slab were determined. The main purpose of this work is to investigate the stability of the response of the numerical slab model to extreme loading conditions. A simplified validation of the numerical model was carried out by analyzing the sensitivity of the model to mass damping. The detailed purpose of the work is to present the results of the displacement and acceleration changes in time, indicating the nature of the dynamic

behavior of the slab. Conclusions were also formulated regarding the requirements for the selection of parameters of the sensors recording both the function of real explosion pressure in time and the function of acceleration in time of the slab model in the intended experimental tests.

2. Computational model of the slab

The subject of the analysis is a steel, rectangular slab with circumferential stiffeners. The dynamic behavior of the slab under the explosive load caused by the detonation of a spherical TNT explosive charge of mass m operating in the free air at a distance r from the center of the slab, is analyzed.

The numerical simulation of the analysed slab is carried out using the Abaqus computational program. In the numerical model, the slab and the circumferential stiffeners were discretized with a shell finite element S4R, i.e. a 4-node, quadrilateral shell element with first-order interpolation, reduced integration, and nine Gaussian points along the cross-section, for displacement and stresses analysis with the large-strain formulation [12].

A fully supported boundary is applied to the slab circumferential stiffeners. The degrees of freedom of movement of all nodes in the bottom layers of the circumferential stiffeners are modeled as limited.

The mesh size of the slab model was dependent on the geometry of the flat slab part in combination with circumferential stiffeners. Number of 30×20 finite elements of a 50×50 mm mesh grid dimensions was used along longitudinal and transverse direction of the slab.

The FE model of the slab is shown in the Fig. 1.

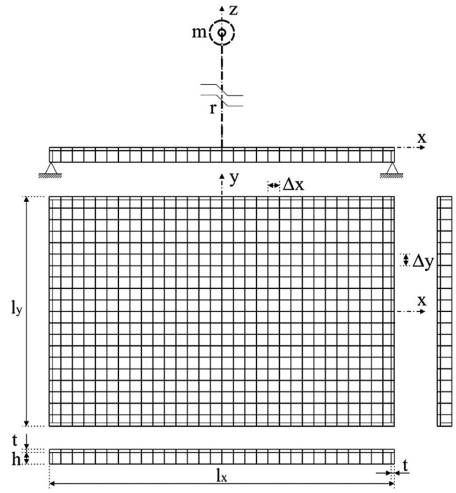

Fig. 1. Geometry details and the finite elements grid of the slab's model

In the numerical analysis the following modelling parameters for the slab under explosive loading were applied, Table 1.

Table 1. Modelling parameters for the slab

Explosive loading	TNT spherical charge mass	$m = 1.5$ kg
	distance from the center of the explosion	$r = 1.0$ m
Material of slab	type of steel	S235
Geometry and FE mesh of slab	length	$l_x = 1.5$ m
	width	$l_y = 1.0$ m
	sheet thickness	$t = 0.012$ m
	circumferential stiffener cross section height	$h = 0.05$ m
	length and width of the FE mesh	$\Delta x = \Delta y = 0.05$ m

The previous experience of many researchers indicates that for explosive charges weighing $m \leq 5$ kg, the effect of the post-explosion gas rarefaction process in the air medium, was no longer observed from a distance:

$$r_{\min} = (10 \div 12)\, r_0 \tag{2.1}$$

where: $r_0 = 0.053\sqrt[3]{m}$ is the equivalent radius of the spherical TNT charge.

The distance $r = 1.0$ m assumed for the analysis meets the condition of the impact of a free shock wave in the air on the slab, without the influence of the pressure of post-explosion rarefied gases from the explosion of a charge with mass of $m = 1.5$ kg, because $r = 16.5 r_0 > r_{\min}$.

3. Modelling of blast load action on slab

3.1. Parameters of blast wave from explosive charge detonation

The distribution of pressure wave change over time from explosive charge detonation is shown in the Fig. 2, see Sochet et al. [3], Karlos and Solomos [1], Siwiński and Stolarski [4].

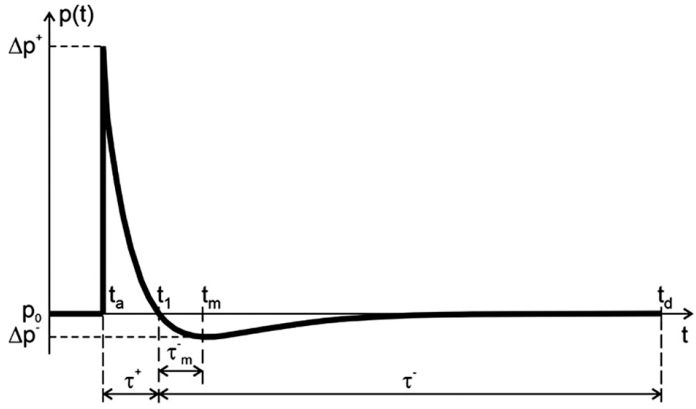

Fig. 2. Pressure wave change over time

www.czasopisma.pan.pl PAN POLSKA AKADEMIA NAUK www.journals.pan.pl

This diagram presents the following parameters characterizing the blast wave:
t_a – arrival time of the wave-front,
Δp^+ – maximum overpressure above atmospheric pressure p_0,
τ^+ – duration of the overpressure phase,
$t_1 = t_a + \tau^+$ – time of decay of the overpressure phase,
Δp^- – minimum depression below atmospheric pressure,
τ_m^- – negative pressure phase duration to reach the minimum depression,
τ^- – duration of the negative pressure phase,
$t_d = t_1 + \tau^-$ – decay time of the negative pressure phase, equivalent to the duration of the pressure load.

The basic parameters characterizing the blast wave in the overpressure phase were determined under assumption that the detonation of explosive TNT spherical charge of mass m [kg] is acting in free air at the distance r [m] from the center of the explosion, for the equivalent distance Z [m·kg$^{-1/3}$]:

$$Z = \frac{r}{\sqrt[3]{m}} \tag{3.1}$$

The maximum overpressure of incident wave Δp_i^+ [bar = 10^5Pa] is determined in the form [3]:
for $0.3 < Z < 2$:

$$\Delta p_i^+ = \exp(2.2411 - 2.3065 \ln Z - 0.3646 \ln^2 Z) \tag{3.2a}$$

for $2 < Z < 30$:

$$\Delta p_i^+ = \exp(2.466 - 3.1974 \ln Z + 0.5375 \ln^2 Z + 0.0024 \ln^3 Z - 0.0096 \ln^4 Z) \tag{3.2b}$$

In turn, the duration of the overpressure phase τ^+ [ms] is specified in the form [3]:
for $0.4 \leq Z \leq 1$:

$$\tau^+ = \sqrt[3]{m} \exp(0.5810 - 0.5423 \ln Z - 11.1572 \ln^2 Z - 11.9941 \ln^3 Z - 3.4023 \ln^4 Z) \tag{3.3a}$$

for $1 < Z \leq 30$:

$$\tau^+ = \sqrt[3]{m} \exp(0.5511 + 0.0271 \ln Z + 0.4937 \ln^2 Z - 0.2079 \ln^3 Z + 0.0268 \ln^4 Z) \tag{3.3b}$$

The incident wave front speed can be determined on the basis of the equation according to Krzewiński [9]:

$$U = \sqrt{a_0^2 + \frac{\Delta p_i^+ (\alpha_Q + 1)}{2\rho_0}} \tag{3.4}$$

where: $a_0 = 340.3$ m/s is the sound speed in the air, $\rho_0 = 1.227$ kg/m^3 is the medium density of dry air, $\alpha_Q \in (1.2, 1.4)$ is the coefficient depending on the specific heat of explosion, which for TNT is equal to $Q = 4200$ kJ/kg [11].

The arrival time of the wave front is defined as:

$$t_a = \frac{r}{U} \tag{3.5}$$

In case of the blast wave impact on the barrier, it is necessary to determine the overpressure on the front of the reflected wave from the barrier in the form [1,4]:

$$\Delta p_r^+ = 2\Delta p_i^+ + \frac{6(\Delta p_i^+)^2}{\Delta p_i^+ + 7p_0} = 2\Delta p_i^+ \frac{4\Delta p_i^+ + 7p_0}{\Delta p_i^+ + 7p_0} \tag{3.6}$$

where: $p_0 = 101325$ Pa is the value of normal ambient atmospheric pressure.

The remaining parameters of the blast wave were determined as the function of pressure wave variability over time using the expression proposed by Lee and Chiu [10], see also [4]:

$$p(t) = \Delta p_r^+ \left(1 - \frac{t}{\tau^+}\right) e^{\left(-\frac{at}{\tau^+}\right)}, \quad a = 1.39(\Delta p_i^+)^{0.54} \tag{3.7}$$

Thus, based on Eq. (3.7), the minimum depression below atmospheric pressure and negative pressure phase duration to reach the minimum depression are determined as follows:

$$\Delta p^- = \frac{1}{a} e^{-(1+a)} \Delta p_r^+ \tag{3.8}$$

and

$$\tau_m^- = \frac{1}{a} \tau^+ \tag{3.9}$$

The duration of the negative pressure phase was also determined by Eq. (3.7) at the assumption that the virtually negligible depression value:

$$\Delta p(t_{dc}) = \varepsilon_a \Delta p^- \tag{3.10}$$

is reached at the conventional decay time t_{dc} of the negative pressure phase with an accuracy equal to, for example, $\varepsilon_a = 0.05$ and t_{dc} is specified assuming $t_a = 0$.

For this purpose, Eq. (3.7) with (3.8) and (3.10) has been transformed into the parametric form:

$$\varepsilon_a \frac{1}{a} e^{-(1+a)} e^{\left(\frac{at_{dc}}{\tau^+}\right)} = 1 - \frac{t_{dc}}{\tau^+} = \delta, \quad \delta < 0 \tag{3.11}$$

The solution of Eq. (3.11) leads to the determination of both the duration of negative pressure phase (exactly):

$$\tau^- = \frac{1}{a} \ln\left(\frac{|\delta| ea}{\varepsilon_a}\right) \tau^+ = -\delta\tau^+ \tag{3.12}$$

and the δ parameter (in the iterative process):

$$\delta = -\frac{1}{a} \ln\left(\frac{|\delta| ea}{\varepsilon_a}\right) \tag{3.13}$$

For the purposes of numerical analysis, the following parameters of the blast wave from explosive charge were calculated, Table 2.

The final, calculated pressure wave change over time for the explosive charge data used is shown in the Fig. 3.

Table 2. Parameters of the blast wave

maximum overpressure above atmospheric pressure p_0	$\Delta p_r^+ = 7.471$ MPa
minimum depression below atmospheric pressure	$\Delta p^- = -0.355$ MPa
virtually negligible depression value	$\Delta p\,(t_{dc}) = -0.0178$ MPa
duration of the overpressure phase	$\tau^+ = 1.848$ ms
negative pressure phase duration to reach the minimum depression	$\tau_m^- = 1.166$ ms
duration of the negative pressure phase to reach the virtually negligible depression value	$\tau^- = 6.695$ ms
conventional time of decay of the negative pressure phase	$t_{dc} = 8.543$ ms

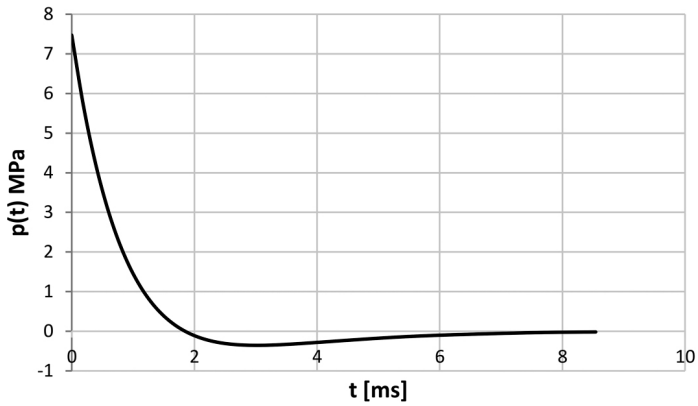

Fig. 3. Calculated pressure wave change over time

3.2. Distribution of the explosion pressure on the slab surface

Detonation of explosive TNT spherical charge of mass m at a distance r from the center of the slab was considered in the arrangement shown in the Fig. 4.

Figure 4 shows the slab load zones described by the corner point $A(xy)$ located at the shortest distance from the slab center $A\,(0, 0)$:

$$A\,(x, y) = A\left\{\begin{array}{llll} x = (i-1)Dx & Dx = \dfrac{l_x}{2I} & i = 1, I \\ y = (j-1)Dy & Dy = \dfrac{l_y}{2J} & j = 1, J \end{array}\right\} \tag{3.14}$$

where: I, J, Dx, Dy are the number and dimensions of the load zones in the appropriate directions of slab division.

www.czasopisma.pan.pl PAN POLSKA AKADEMIA NAUK www.journals.pan.pl

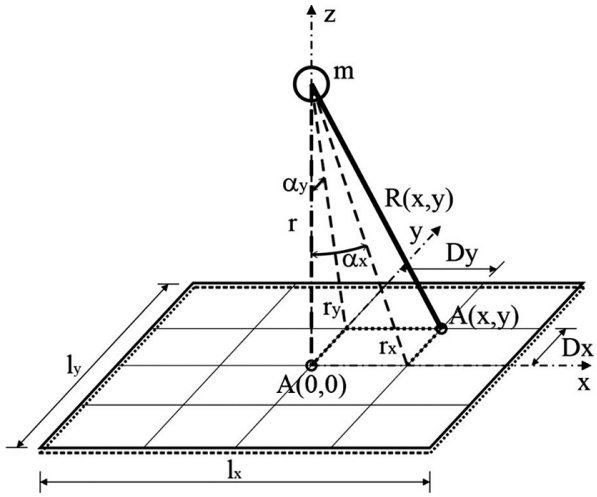

Fig. 4. Location of the explosive charge in relation to any point on the slab surface (description in the text)

In turn, the distance of the explosive charge from each load zone is defined as follows:

$$R(xy) = \frac{r}{\cos\alpha_x \cos\alpha_y} \tag{3.15}$$

where: $\alpha_x = \text{arctg}\,\frac{x}{r}, \alpha_y = \text{arctg}\,\frac{y}{r}$ are the appropriate angles of wave front incident on the slab.

Thus, the blast wave parameters described by Eq. (3.1)–(3.10) are determined separately for each load zone. To this purpose, it was assumed that these parameters depend on the distance (3.15) from the slab load zone to the explosive charge and they are constant over the entire area of the zone.

However, the explosion pressure distribution on the slab surface can be determined in a simplified way. For this purpose, the overpressure on the reflected wave front at any point of the slab $A(xy)$ located at a distance $R(xy)$ from the explosive charge is described as follows:

$$\Delta p_r^+(R) = \Delta p_r^+(r)\cos^2\alpha_x \cos^2\alpha_y = \Delta p_r^+(r)\, C_{xy} \tag{3.16}$$

where: $\Delta p_r^+(r) = \Delta p_r^+$ is the value of overpressure on the reflected wave front at the distance of the charge from the slab $r = R(0,0)$ determined according to Eq. (3.6), $C_{xy} = \cos^2\alpha_x \cos^2\alpha_y$ are the coefficients of the explosion pressure distribution for each slab load zone.

Also, the arrival time of the wave front to any point of the slab $A(xy)$ is now described according to (3.5) but with the distance $R(xy)$ and with the modified value of overpressure (3.16) taken into account:

$$t_a = \frac{R(x,y)}{U\left[\Delta p_r^+(R)\right]} \tag{3.17}$$

For the purposes of numerical analysis, the uniform explosion pressure distribution on the slab was assumed. In this case the arrival time of the wave front to the center point of the slab is equal to $t_a = 0.873$ ms.

www.czasopisma.pan.pl PAN POLSKA AKADEMIA NAUK www.journals.pan.pl

4. Dynamic equilibrium equation

The dynamic equilibrium equation of the slab at the current time t, was applied in the form:

$$\boldsymbol{M}\ddot{\boldsymbol{w}}(t) + \boldsymbol{C}\dot{\boldsymbol{w}}(t) + \boldsymbol{K}\boldsymbol{w}(t) = \boldsymbol{P}(t) \tag{4.1}$$

where: $\boldsymbol{M}, \boldsymbol{C}$, and $\boldsymbol{K}$ are the nodal mass, damping, and stiffness matrices, $\ddot{\boldsymbol{w}}(t)$, $\dot{\boldsymbol{w}}(t)$, and $\boldsymbol{w}(t)$ are the nodal accelerations, velocities and displacements vectors, $\boldsymbol{P}(t)$ is the vector of the external applied forces.

The Rayleigh model of damping was assumed that the damping matrix is a linear combination of the mass and stiffness matrices:

$$\boldsymbol{C} = \alpha\boldsymbol{M} + \beta\boldsymbol{K} \tag{4.2}$$

where: α and β are assumed damping parameters.

In the numerical analysis, only the Rayleigh mass damping parameter α was used, omitting the β parameter. The parameter α was chosen in such a way as to define the damped aperiodic motion, which disappears after reaching 5 to 10 maximum displacement amplitudes. The mass damping parameter was analyzed in the range $\alpha = [0; 110]$.

The explicit procedure was used for solving of equation of motion (4.1) under assumption of the lumped mass matrix of diagonal structure [15]. Then, the accelerations at the beginning of the current time are calculated as:

$$\ddot{\boldsymbol{w}}(t) = \boldsymbol{M}^{-1}\left[\boldsymbol{P}(t) - \boldsymbol{C}\dot{\boldsymbol{w}}(t) - \boldsymbol{K}\boldsymbol{w}(t)\right] \tag{4.3}$$

The central difference scheme is used to explicit time integration the equations of motion. Within this scheme the velocities and the displacements are determined at the end of the next time increment $t + \Delta t$ knowing all the kinematic conditions from the previous increments:

$$\dot{\boldsymbol{w}}(t + \Delta t) = \dot{\boldsymbol{w}}(t - \Delta t) + 2\Delta t\ddot{\boldsymbol{w}}(t) \tag{4.4}$$

$$\boldsymbol{w}(t + \Delta t) = \boldsymbol{w}(t) + \Delta t\frac{\dot{\boldsymbol{w}}(t + \Delta t) + \dot{\boldsymbol{w}}(t)}{2} \tag{4.5}$$

The initialization the central difference scheme requires to introduce the initial conditions at the time $t_0 = 0$.

$$\ddot{\boldsymbol{w}}(t_0) = \ddot{\boldsymbol{w}}_0, \quad \dot{\boldsymbol{w}}(t_0) = \dot{\boldsymbol{w}}_0, \quad \dot{\boldsymbol{w}}(t_0 - \Delta t) = \dot{\boldsymbol{w}}_0 - \Delta t\ddot{\boldsymbol{w}}_0 \tag{4.6}$$

where: the Eq. $(4.6)_3$ follows on the first order accurate Taylor series expansion for the velocities.

Since the explicit method for integration the equations of motion is conditionally stable, it is necessary to introduce the time step limitation in relation to the critical time step:

$$\Delta t \leq r\Delta t_{\text{crit}} \tag{4.7}$$

where: $0.2 \leq r \leq 0.9$ is the assumed reduction factor depending on the nonlinearity level of the problem under consideration.

The critical time step is the function of the element length and the wave velocity of the material:

$$\Delta t_{\text{crit}} = \frac{\Delta L^e_{\min}}{c_{d,\max}} \tag{4.8}$$

where: $\Delta L^e_{\min}$ is the smallest characteristic length of the element in the FE-discretization, $c_{d,\max} = \sqrt{\frac{E}{\rho}}$ is the fastest dilatation wave velocity in the elastic material, E is Young's modulus, and ρ is the mass density.

5. Material model

The slab and circumferential stiffeners are made from low carbon mild steel. In numerical analysis, the Huber–Mises–Hencky yield surface with the associated flow rule is used in the Johnson–Cook plasticity model.

The Johnson–Cook constitutive equation is used to describe the evolution of the combined effects of isotropic plastic hardening in strain rate and temperature dependence as the basic material behavior of the material in the form [13, 14]:

$$\sigma_{yd} = \left[A + B\left(\varepsilon^{pl}_{\text{eff}}\right)^n\right]\left[1 + Cln\left(\frac{\dot{\varepsilon}^{pl}_{\text{eff}}}{\dot{\varepsilon}_0}\right)\right](1 - \tau^m) \tag{5.1}$$

where: σ_{yd} is the dynamic yield stress (MPa), A is material parameter equal to the initial, static yield stress σ_y (MPa), B is the plastic hardening modulus (MPa), $\varepsilon^{pl}_{\text{eff}}$ is the effective plastic strain; n is the plastic hardening parameter, C is the strain rate hardening parameter, $\dot{\varepsilon}^{pl}_{\text{eff}}$ is effective plastic strain rate (s^{-1}), $\dot{\varepsilon}_0$ is the reference strain rate for which the dynamic yield stress is equal to static yield stress $\sigma_{yd} = \sigma_y$ (s^{-1}), τ is the nondimensional temperature coefficient; m is the temperature softening parameter.

The nondimensional temperature coefficient is defined as:

$$0 < \tau = \frac{T - T_{\text{trans}}}{T_{\text{melt}} - T_{\text{trans}}} < 1 \tag{5.2}$$

where: T is the current temperature (K) at which the experiment is being carried out, T_{trans} is the transition temperature at or below which the material parameters must be measured, T_{melt} is the is the melting temperature at which the material will be melted and will behave with no shear resistance.

The limitation for τ in (5.2) mean that if $T \leq T_{\text{trans}}$ then $\tau = 0$ or if $T \geq T_{\text{melt}}$ then $\tau = 1$ and $\sigma_{yd} = 0$.

In the numerical analysis, the following parameters for S235 steel were used, describing the adopted Johnson–Cook constitutive model, Table 3.

Table 3. Mechanical properties of the S235 steel and material model parameters

ρ	ν	E	$A = \sigma_y$	B	n	C	$\dot{\varepsilon}_0$	T	T_{trans}	T_{melt}	m
kg/m^3		GPa	MPa	MPa			s^{-1}	K	K	K	
7850	0.3	210	235	130	0.024	0.05	0.00001	293	293	1540	1.03

6. Analysis of the numerical results

The results of the numerical analysis for the slab under the computational load caused by the explosion of the TNT explosive charge with a mass of 1.5 kg at a distance of 1 m are presented. The results illustrate the change in time of the displacement and acceleration of the slab midpoint caused by the pressure load of the blast shock wave.

The results are presented for two values of the mass damping parameter α. The critical time step for the explicit method of integrating the equations of motion was determined according to Eq. (4.8) and is equal to $\Delta t_{\text{crit}} = 9.967$ μs The total analysis time was assumed to be 50 ms.

Figure 5 shows the results for the parameter $\alpha = 0$, which defines the undamped vibrating motion. The average value of the time step determined in the calculation procedure for this case of analysis is $\Delta t = 8.012$ μs.

The first maximum displacement amplitude is $w_1 = 11.71$ cm and was reached in time $t_1 = 3.708$ ms.

The vibrating motion stabilizes after the 4th maximum displacement amplitude and takes place around the value of the permanent displacement $w_p \cong 10.42$ cm, which is determined when the displacement velocity reaches zero value.

The variability of the midpoint acceleration over time is characterized by large jumps in value during the overpressure wave ($\tau^+ = 1.848$ ms) and at the beginning of the negative pressure wave. The initial (i.e. at the time $t_0 = 0.0$) acceleration value is $\ddot{w}(t_0) = 79315$ m/s^2.

The highest positive acceleration value $\ddot{w}_{\max} = 112142$ m/s^2 was recorded at the time $t = 0.874$ ms. In turn, the smallest negative acceleration value (deceleration) $\ddot{w}_{\min} = -154426$ m/s^2 was recorded at the time $t = 2.595$ ms, i.e. before reaching the first maximum displacement amplitude. In the period of stabilization of the vibrating motion after the 4th maximum displacement amplitude, the acceleration values change in the range $\Delta\ddot{w} \cong (-42000; 29000)$ m/s^2.

The average period of inelastic free vibrations of the slab, recorded after the end of the pressure wave action at the time $t_{dc} = 8.543$ ms, is $T_{f\upsilon} = 5.131$ ms.

Figure 6 presents the results for the parameter $\alpha = 110$ defining the damped vibration motion. The damping parameter was selected in such a way as to define the damped motion that disappears after reaching from 5 to 10 maximum displacement amplitudes.

The average value of the time step determined in the calculation procedure for this case of analysis is $\Delta t = 8.009$ μs.

The first maximum displacement amplitude is $w_1 = 10.28$ cm and was reached in time $t_1 = 2.724$ ms.

The vibrating motion disappears after the 9th maximum displacement amplitude. Differences in displacement amplitudes tend asymptotically to zero at the value of permanent displacement $w_p \cong 8.77$ cm.

As in the case of the undamped motion of the slab, the variability of the midpoint acceleration over time is characterized by large jumps in value during the overpressure wave and at the beginning of the negative pressure wave. The initial acceleration value is the same as in the case of undamped slab motion.

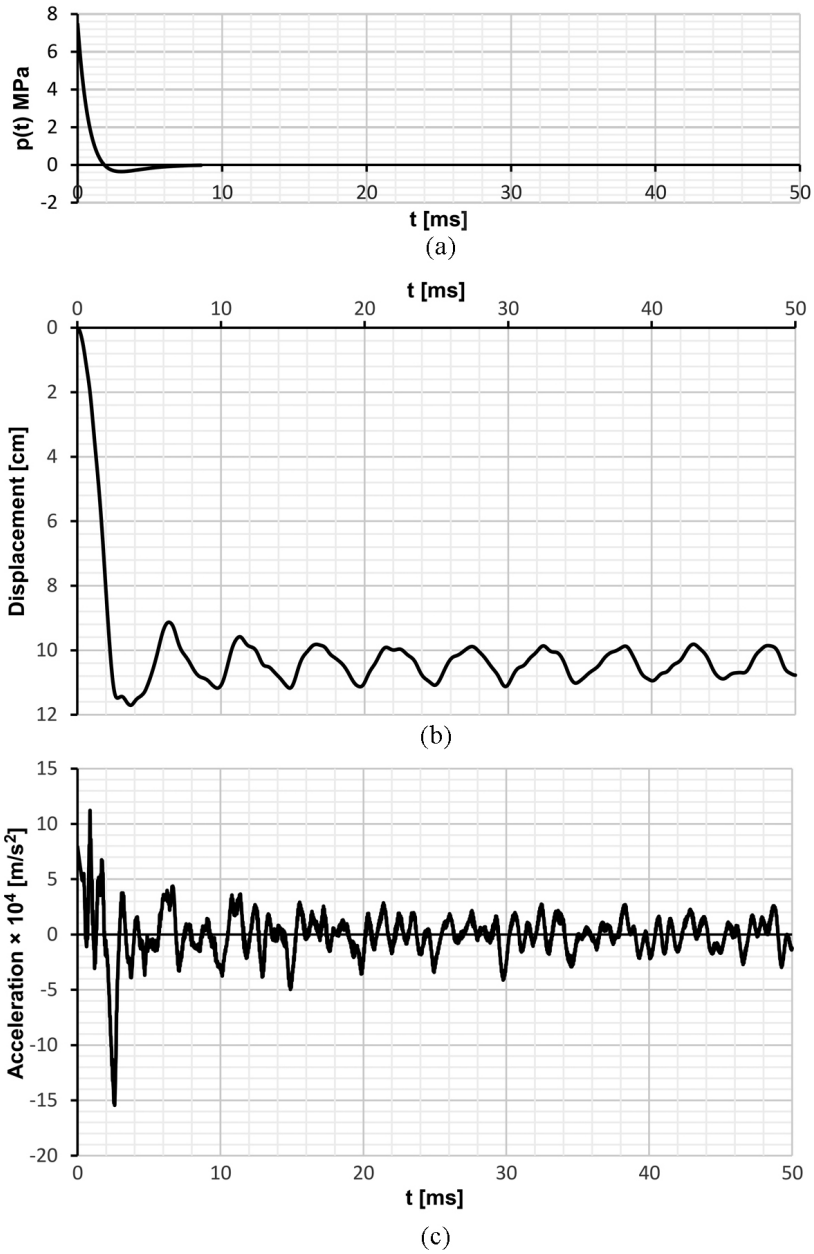

Fig. 5. The results of the numerical analysis for the slab subjected to explosion for the mass damping parameter $\alpha = 0$; (a) change in the pressure wave over time, (b) change in the displacement of the midpoint over time, (c) change in the acceleration of the midpoint over time

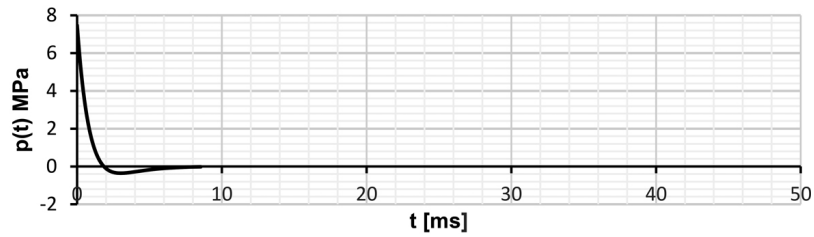

(a)

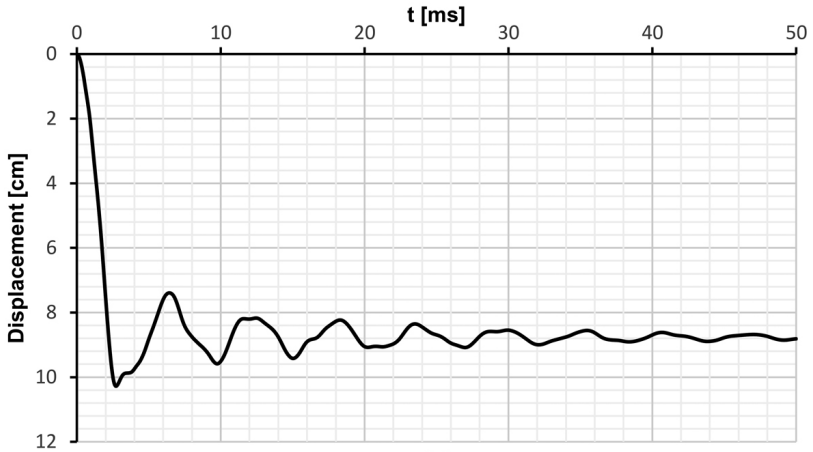

(b)

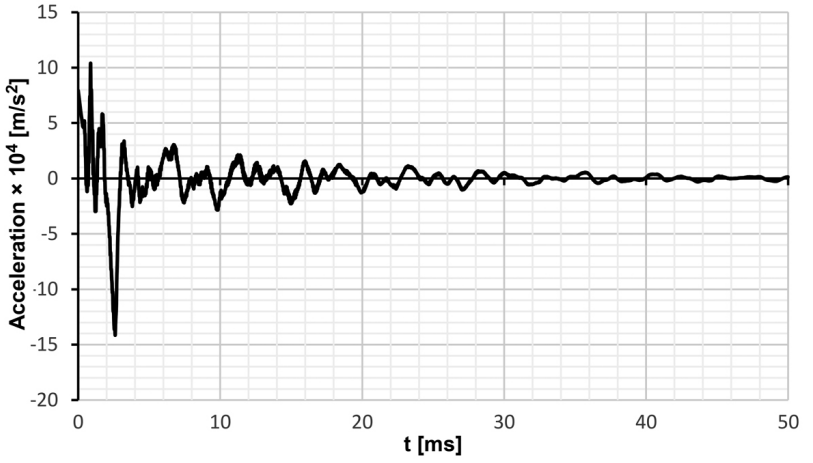

(c)

Fig. 6. The results of the numerical analysis for the slab subjected to explosion for the mass damping parameter $\alpha = 110$; (a) change in the pressure wave over time, (b) change in the displacement of the midpoint over time, (c) change in the acceleration of the midpoint over time

The highest positive acceleration value $\ddot{w}_{\max} = 103956$ m/s^2 was recorded at the time $t = 0.874$ ms. Compared to the case of undamped slab motion, the highest value of positive acceleration is less by about 7.3%, but it was reached in the same time.

The smallest negative acceleration value (deceleration) $\ddot{w}_{\min} = -141458$ m/s^2 was recorded at the time $t = 2.603$ ms, also before reaching the first maximum displacement amplitude. The smallest value of negative acceleration is greater by about 9.2% compared to the case of undamped slab motion and was achieved in a slightly longer time.

The effect of acceleration damping is practically visible already after the 4th maximum displacement amplitude. Then the acceleration amplitudes decrease significantly. After the 9th maximum displacement amplitude, the acceleration values change in the range $\Delta\ddot{w} \cong (-2500; 1400)$ m/s^2, with a constant tendency to reach practically zero values.

7. Conclusions

The paper presents the methodology for determination the numerical prognosis of the dynamic response of the rectangular steel slab subjected to an explosive load.

As a result of the numerical analysis, the results of changes in displacement and acceleration in time were presented, indicating the nature of the dynamic behavior of the slab.

The solution was obtained for specific material and geometrical parameters of the steel slab and for the impact of the pressure wave from the assumed explosive charge of mass $m = 1.5$ kg placed at a distance of $r = 1.0$ m from the slab.

The most important features of the obtained solution are as follows.

1. Numerical solution method:
   - Stability of the response of the numerical slab model to extreme loading conditions was proved
   - Adopted time step of the numerical solution method and the interdependent mesh size guarantee the stability and the effectiveness of the numerical analysis
   - Analysis of the model's sensitivity to mass damping confirmed the stable behavior of the slab.
2. Load variation over time:
   - Very high value of the initial pressure $\Delta p_r^+ = 7.471$ MPa with a rapid decrease in a very short time $\tau^+ = 1.848$ ms of the overpressure phase
   - Very small (but not negligible) value of pressure $\Delta p^- = -0.355$ MPa realized with a slow increase and then - decrease in a relatively long time $\tau^- = 6.695$ ms of the negative pressure phase.
3. Variation of the displacement of the slab midpoint over time in damped motion:
   - Very large value of the first maximum displacement amplitude $w_1 = 10.28$ cm (i.e. of the order of ≈ 8.5 times the plate thickness), reached in time $t_1 = 2.724$ ms
   - Very large value of the permanent displacement $w_p \cong 8.77$ cm, reached after the 9th maximum amplitude of the displacement in the time $t_p \cong 50$ ms.

4. Variation of the acceleration of the slab midpoint over time in damped motion:
   – Very high values of positive acceleration $\ddot{w}_{\max} = 103956$ m/s^2 and negative acceleration $\ddot{w}_{\min} = -141458$ m/s^2 (i.e. of the order of $\approx 10600 g_n$ and $\approx 14400 g_n$, where $g_n = 9.80665$ m/s^2 is the normal gravitational acceleration), achieved in a time shorter than the time of reaching the first maximum displacement amplitude
   – Relatively small acceleration values changing in the range $\Delta\ddot{w} \cong (-2500; 1400)$ m/s^2, (i.e. of the order of $\approx (-255 g_n; 143 g_n)$), reached after the 9th maximum displacement amplitude.

Such characteristics of short-term phenomena make it necessary to carefully select the type of sensors that record the parameters of the load and movement of the experimental model of the slab. Assuming that these sensors will be permanently fixed in the zone of the midpoint of the slab, they must be able to record measurements under conditions of very large acceleration changes.

Recording the actual change of the pressure wave over time directly on the slab surface will allow verification of the pressure value of the wave reflected from the slab, which is not a completely rigid barrier. Moreover, the registration of changes of acceleration over time will make it possible to determine the displacement velocity and the displacement of a specific point on the slab. As a consequence, it will be possible to precisely identify the parameters of the numerical model simulating the dynamic behavior of the steel slab under explosive load.

References

[1] Joint Research Centre, Institute for the Protection and Security of the Citizen, V. Karlos, B. Viaccoz, and G. Solomos, *Calculation of Blast Loads for Application to Structural Components*. Publications Office of the EU, 2013, doi: 10.2788/61866.

[2] W.A. Trzciński, "A Review of Methods for Calculation of Blast Wave Parameters", *Problems of Mechatronics. Armament, Aviation, Safety Engineering*, vol. 7, no. 1, pp. 61–78, 2016, doi: 10.5604/20815891.1195201 (in Polish).

[3] I. Sochet, D. Gardebas, S. Calderara, Y. Marchal, and B. Longuet, "Blast Wave Parameters for Spherical Explosives Detonation in Free Air", *Open Journal of Safety Science and Technology*, vol. 1, no. 2, pp. 31–42, 2011, doi: 10.4236/ojsst.2011.12004.

[4] J. Siwiński and A. Stolarski, "Analysis of the external explosion action on the building barriers", *Bulletin of Military University of Technology*, vol. 64, no. 2, pp. 173–196, 2015, doi: 10.5604/12345865.1157340 (in Polish).

[5] T. Niezgoda, G. Sławiński, R. Gieleta, and M. Świerczewski, "Protection of military vehicles against mine threats and improvised explosive devices", *Journal of KONBiN*, no. 1, pp. 123–134, 2015.

[6] J. Trajkovski, J. Perenda, and R. Kunc, "Blast response of Light Armoured Vehicles (LAVs) with flat and V-hull floor", *Thin-Walled Structures*, vol. 131, pp. 238–244, 2018, doi: 10.1016/j.tws.2018.06.040.

[7] B.-W. Park and S.-R. Cho, "Simple design formulae for predicting the residual damage of unstiffened and stiffened plates under explosion loadings", *International Journal of Impact Engineering*, vol. 32, no. 10, pp. 1721–1736, 2006, doi: 10.1016/j.ijimpeng.2005.01.005.

[8] C. Zheng, X. Kong, W. Wu, and F. Liu, "The elastic-plastic dynamic response of stiffened plates under confined blast load", *International Journal of Impact Engineering*, vol. 95, pp. 141–153, 2016, doi: 10.1016/j.ijimpeng.2016.05.008.

[9] R. Krzewiński, *Dynamics of explosion. Part I: Method of load determining, Part II: Action of explosion in inertial media*. Warsaw, Poland: Military University of Technology Publishing, 1982, 1983 (in Polish).

[10] J.H.S. Lee, *Physics of explosion*. Montreal: McGill University, 1984.

www.czasopisma.pan.pl PAN POLSKA AKADEMIA NAUK www.journals.pan.pl

[11] S. Cudziło, A. Maranda, J. Nowaczewski, R. Trębiński, and W.A. Trzciński, *Military explosives*. Publishing House of the Faculty of Metallurgy and Materials Engineering of the Czestochowa University of Technology, 2000 (in Polish).

[12] *ABAQUS Analysis User's Manual, Version 6.5*. Providence, RI, USA: Abaqus Inc., 2004.

[13] G.R. Johnson and W.H. Cook, "A constitutive model and data for metals subjected to large strain, high strain rates and high temperature", in *Proceedings of the 7th International Symposium on Ballistics*, *19-21 April 1983.* Hague, Netherlands, 1983, pp. 541–547.

[14] G.R. Johnson and W.H. Cook, "Fracture Characteristics of Three Metals Subjected to Various Strains, Strain rates, Temperatures and Pressures", *Engineering Fracture Mechanics*, vol. 21, no. 1, pp. 31–48, 1985, doi: 10.1016/0013-7944(85)90052-9.

[15] P. Wriggers, *Nonlinear Finite Element Methods*. Berlin/Heidelberg, Germany: Springer, 2008.

Numeryczna prognoza dynamicznej reakcji stalowej płyty prostokątnej obciążonej wybuchowo

Słowa kluczowe: analiza numeryczna, obciążenie wybuchowe, płyta stalowa, proces dynamicznej deformacji, tłumienie

Streszczenie:

W artykule przedstawiono metodykę wyznaczania numerycznej prognozy reakcji dynamicznej prostokątnej płyty stalowej poddanej obciążeniu wybuchem, mającą na celu dokładne przygotowanie badań eksperymentalnych. W prezentowanej pracy zastosowano odpowiednią kombinację wzorów znanych z literatury, aby w pełni opisać parametry oddziaływania fali uderzeniowej na płytę stalową. W celu opisania zachowania dynamicznego prostokątnej płyty stalowej wykorzystano zasoby programu obliczeniowego ABAQUS. Do opisu dynamicznego zachowania się materiału konstrukcyjnego zastosowano model konstytutywny Johnsona–Cooka. Zastosowano jawną procedurę rozwiązania równania ruchu płyty. Wyznaczono parametry fali uderzeniowej od wybuchu ładunku trotylu o założonej masie oraz odległości jego położenia od płyty. W wyniku analizy numerycznej przedstawiono wyniki zmian przemieszczeń i przyspieszeń w czasie, wskazując na charakter bardzo intensywnego i szybkozmiennego zachowania dynamicznego płyty. Sformułowano również wnioski dotyczące wymagań dotyczących doboru parametrów czujników rejestrujących zarówno funkcję rzeczywistego ciśnienia wybuchu w czasie, jak i funkcję przyspieszenia w czasie modelu płyty podczas badań eksperymentalnych.

Received: 2024-01-26, Revised: 2024-04-23